Charge trapping-detrapping mechanism of barrier breakdown in MgO magnetic tunnel junctions

S. Amara-Dababi, R. C. Sousa, M. Chshiev, H. Béa' , J. Alvarez-Hérault, L. Lombard, I. L. Prejbeanu, K. Mackay, and B. Dieny

Citation: Appl. Phys. Lett. **99**, 083501 (2011); doi: 10.1063/1.3615654
View online: http://dx.doi.org/10.1063/1.3615654
View Table of Contents: http://aip.scitation.org/toc/apl/99/8
Published by the American Institute of Physics

Charge trapping-detrapping mechanism of barrier breakdown in MgO magnetic tunnel junctions

S. Amara-Dababi,[1] R. C. Sousa,[1] M. Chshiev,[1] H. Béa,[1,a)] J. Alvarez-Hérault,[2] L. Lombard,[2] I. L. Prejbeanu,[2] K. Mackay,[2] and B. Dieny[1]
[1]*SPINTEC, UMR CEA/CNRS/UJF-Grenoble 1/Grenoble-INP, INAC, Grenoble F-38054, France*
[2]*Crocus Technology, Grenoble, France*

(Received 20 May 2011; accepted 24 June 2011; published online 22 August 2011)

Endurance of MgO-based magnetic tunnel junctions has been studied using a time-dependent dielectric breakdown method. Series of successive electrical pulses were applied until electrical breakdown of the tunnel barrier. We show that two electrical breakdown regimes exist depending on the time interval Δt between pulses compared to a characteristic escape time of trapped electrons $\tau_0 \sim 100$ ns. For $\Delta t < \tau_0$, breakdown is caused by a high average charge trapped in the barrier. For $\Delta t > \tau_0$, breakdown is ascribed to large temporal modulation of trapped charges causing alternating stress in the barrier oxide. Between these two regimes, the tunnel junctions reach a very high endurance. © *2011 American Institute of Physics*. [doi:10.1063/1.3615654]

Spin transfer torque magnetoresistive random access memory (STT-MRAM) are promising memory technologies because of their non-volatility, high speed operation, low power consumption, very large endurance, high density, and compatibility with standard complementary metal oxide semi-conductor (CMOS) process.[1] As the magnetic tunnel junction (MTJ) size shrinks, the MTJ resistance must remain comparable to the resistance of the selection transistor in a one transistor-one MTJ (1T-1MTJ) design. Hence, a thinner tunnel barrier that does not compromise on reliability is required. This is even more important for STT-MRAM technologies as compared to field switching MRAMs since a large current flow through the barrier is necessary for writing. Oxide barrier breakdown represents one of the main reliability issues for advanced semiconductor memory technology. Despite numerous studies on the tunnel magnetoresistance (TMR) of MgO-based MTJs,[1–8] the breakdown mechanism of ultrathin MgO-based MTJ has not been thoroughly investigated. A more detailed understanding of MTJ reliability issues is still essential for the success of STT-MRAMs or of other devices based on hybrid CMOS/MTJ technology.

Lifetime of MTJs is usually measured using a time dependent dielectric breakdown[3,4] technique carried out by applying a DC voltage while recording the time to breakdown. However, the normal operation conditions of an MTJ in a MRAM device require applying a large number of read/write voltage pulses a few nanoseconds long.

This work reports on the breakdown behavior of MgO-based MTJs submitted to successive voltage pulses. We studied their endurance as a function of the time interval between pulses as well as pulses amplitude and polarity. An earlier study has shown that MgO dielectric breakdown measurements carried under DC voltage and under cumulative pulsed voltage yield equivalent results for pulse-widths longer than 100 ns.[7] In the present study, we chose to work with shorter constant pulse-width of $\tau = 30$ ns which is close to the normal operating conditions. A very peculiar behavior was observed characterized by a very large enhancement of the MTJ endurance around an intermediate characteristic time interval Δt between successive pulses of the order of 100 ns. We ascribe this behavior to charging/discharging effects within the MgO barrier due to the presence of interfacial and/or bulk electron traps in the MgO layer.

The junctions studied had the following composition: buffer/PtMn 20/CoFe 2/Ru 0.8/CoFeB 2/Mg 1.1 plasma ox/CoFeB 2/NiFe 3/cap (thicknesses in nm). The MgO barrier was prepared by plasma oxidation of an Mg layer. The measured devices were patterned into 250 nm circular pillars showing 100%–130% TMR ratio and a resistance area (RA) product of 30 $\Omega \cdot \mu m^2$ except otherwise mentioned.

The experimental procedure consisted in applying successive pulses of 30 ns with constant amplitude (1.30 V–1.80 V) at zero magnetic field until barrier breakdown occurs. The pulse amplitude was corrected taking into account the voltage drop in the electrical leads. The latter was determined for every junction from the resistance value after breakdown as shown in Figs. 1(a) and 1(b). No gradual degradation of the barrier resistance was observed. The breakdown occurs abruptly as shown in Fig. 1(b) and corresponds to a sharp drop of the junction resistance accompanied by a degradation of the TMR response (Fig. 1(a)). The time interval, i.e., the delay, between consecutive pulses (Δt) was chosen as a variable parameter. Experiments were repeated for time delays between pulses from 1 ns up to 10 μs. Furthermore, the experiments were performed in accelerated breakdown conditions, i.e., with a corrected pulse amplitude ranging between 1.0 V and 1.5 V, corresponding to an electric field of ~9–14 MV/cm. This pulse amplitude is two to three times higher than that required for STT-MRAM writing under normal operation conditions.

For each value of pulse amplitude and delay between pulses Δt, the distribution of number of applied pulses leading to breakdown was determined from measurements performed on a set of 20–40 junctions. It is well described by a Weibull distribution with a cumulative distribution F as function of time (see Fig. 2(a)) given by

a)Electronic mail: helene.bea@cea.fr.

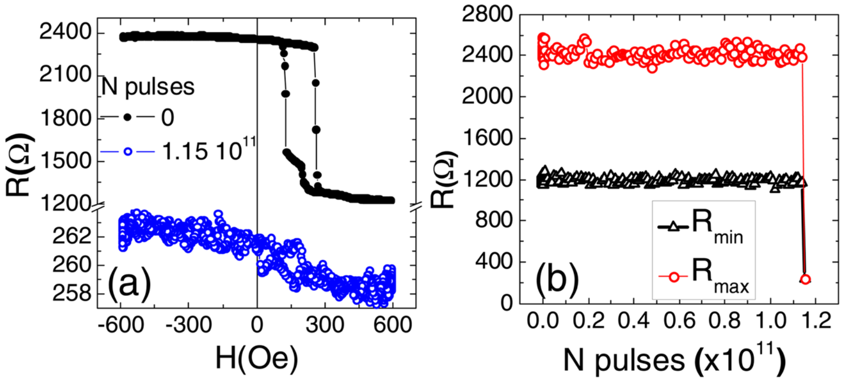

FIG. 1. (Color online) (a) TMR curves before (top loop) and after breakdown (bottom loop). For this junction, breakdown occurred after 1.15×10^{11} pulses of $+1.3$ V amplitude separated by a delay of 100 ns. (b) Evolution of R_{min} (parallel magnetic configuration) and R_{max} (antiparallel magnetic configuration) vs number of pulses. A sharp drop of R_{min} and R_{max} is observed after 1.15×10^{11} pulses when the breakdown abruptly occurs. The time interval and voltage used here were 100 ns and $+1.3$ V.

$$F(t) = 1 - \exp\left[-\left(\frac{t}{\eta}\right)^{\beta}\right].$$

This distribution is characterized by two parameters: (1) the shape parameter β, associated with the breakdown mechanism, and (2) the scale parameter η, representing the number of pulses after which a fraction 63.2% of MTJs has failed.

For a fixed Δt of 100 ns, we studied the voltage dependence of η by stressing the MTJs with various pulse amplitudes of positive polarity (from 1.20 to 1.35 V) in the magnetic antiparallel state. The dependencies obtained are plotted in Fig. 2(b). The η variation was fitted to the E-model where log(η) is proportional to the electric field (E).[3] This extrapolation tends to indicate clearly that, for these pulse conditions with an operating voltage of 0.4 V to 0.7 V typically used in STT-MRAM, the MTJs endurance can reach values over 10^{16} cycles required for use as core level memories with 10 year lifetime.

We then studied the evolution of η as a function of the delay Δt between successive pulses (Fig. 3). As explained above, each point is derived from endurance measurements on a set of 20–40 junctions. This experiment shows that the η variation exhibits two different regimes separated by a pronounced maximum for unipolar pulses. For short delays between pulses (1 ns $< \Delta$t $<$ 100 ns), the barrier lifetime increases dramatically with Δt from rather short values for Δt $<$ 30 ns to values 4 to 10 orders of magnitude larger when Δt approaches $\sim$100 ns. When the delay Δt is longer than 100 ns, the opposite evolution is observed: the barrier lifetime

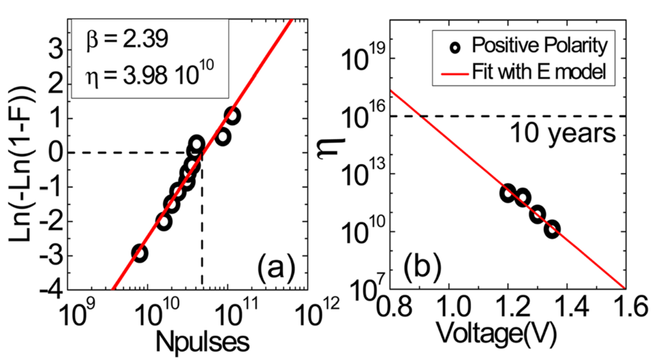

FIG. 2. (Color online) (a) Weibull plot of the number of pulses to dielectric breakdown for V = 1.30 V and Δt = 100 ns. The fitted η and β parameters are given. (b) Variation of η versus applied pulses voltage for Δt = 100 ns. Data were extrapolated to determine the MTJs lifetime for 0.8 V pulses corresponding to an upper limit of write conditions in STT-MRAM applications.

decreases as the time between consecutive pulses increases and asymptotically reaches a value of the same order of magnitude as for short Δt in the range of investigated voltage.[9] Such behavior was observed for both pulse polarities (either positive or negative pulses) and for different pulse amplitudes with the η maximum strongly depending on the amplitude of the voltage pulses (Figs. 3(b) and 3(c)). However, remarkably, the peak completely disappears when pulses of alternating polarity are used, as shown in Fig. 3(a) (up triangles).

Because of the marked difference between pulses of the same and opposite polarity, these observations cannot be explained by only a heating effect in the tunnel barrier. Rather, we developed an interpretation in terms of charge trapping/detrapping effect based on qualitative representations of the population of trapped electrons in the barrier as represented in Figs. 3(d)–3(f). At each pulse, some of the tunneling electrons get trapped in the barrier at trapping sites. These trapping sites could be oxygen vacancies or interfacial traps caused either by boron oxide formation next to the MgO barrier due to B diffusion towards the MgO barrier or dislocations resulting from the 4% crystallographic mismatch[10] between MgO and CoFe. Then between two pulses, the trapped electrons may escape from their traps with a characteristic time τ_0 (which is $\sim$100 ns in our experiments). In addition, when an electron gets trapped in the barrier, a screening positive charge appears in the metallic electrodes yielding a large electrostatic force between these two opposite charges. This force is estimated to be $\sim$10 nN assuming that the distance between charges is half the barrier thickness. This attractive force translates into a local compressive stress exerted on the barrier. In order to estimate the corresponding MgO lattice distortion, we first derive an order of magnitude of the MgO lattice stiffness constant k from typical phonon frequency in MgO of $f = 10$ THz and by considering the reduced mass of MgO ($m = 4.05 \times 10^{-26}$kg). The calculated value is then $k = (2\pi f)^2 m = 160$ kg/s^2. The 10 nN force then yields a lattice distortion of the order of $\Delta x = 0.056$ Å. This value is the same order of magnitude as the typical amplitude of vibration of atoms at room temperature in a crystal such as MgO (0.1 Å).

The three regimes are then interpreted as follows: (1) The first observed regime corresponds to Δt $\ll \tau_0$. At each pulse, the barrier gets more and more charged up to an asymptotic regime characterized by a high density of trapped electrons. The barrier is then submitted to a large stress which renders it more fragile. As a result, its lifetime is

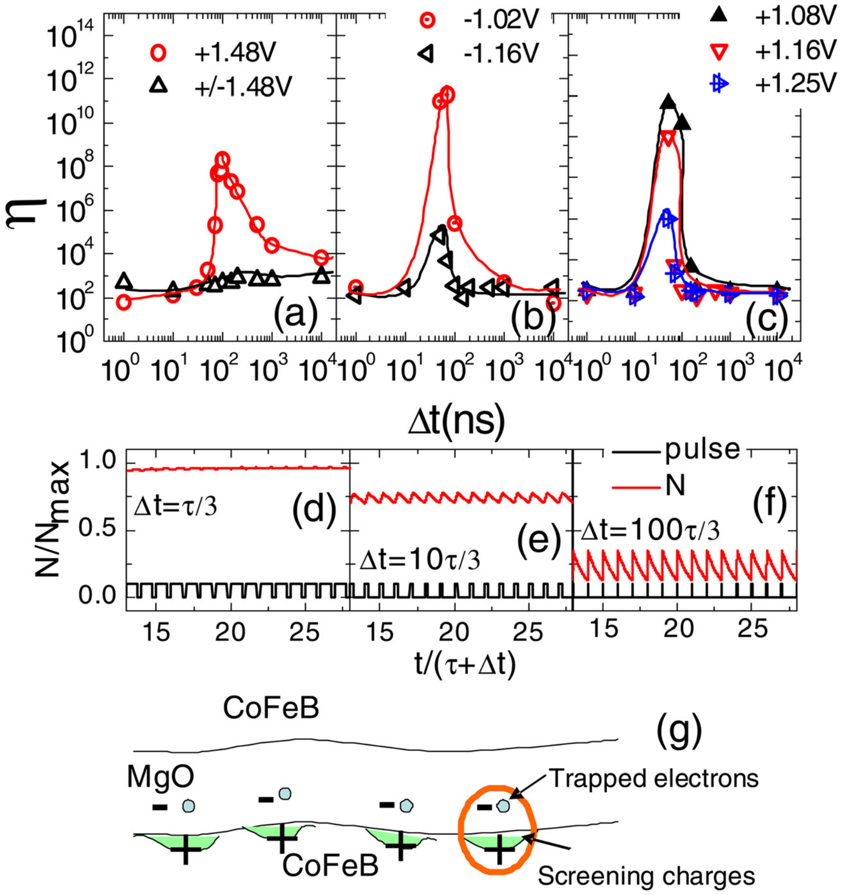

FIG. 3. (Color online) Evolution of η as a function of delay between pulses, with unipolar positive or bipolar pulses (a), with negative (b) and positive (c) pulses of various amplitudes. The lines are guides to the eye. Studied samples have different RA product of 47 (a) and 30 $\Omega\ \mu m^2$ (b-c). (d)-(f) Qualitative representation of the time variation of the normalized population of trapped electrons in steady state. On the horizontal axis, the time is normalized by the signal period, i.e., $\tau + \Delta t$ (pulse duration + delay). (d), (e), and (f) cases correspond, respectively, to short/intermediate/long delays between pulses. (g) Schematic representation of trapped electrons in the barrier screened by positive image charges in electrodes. The circle indicates the charges in strong electrostatic interaction generating a large local compressive stress on the barrier.

decreased yielding the low η value observed for short Δt. (2) In the opposite limit $\Delta t \gg \tau_0$, some of the tunneling electrons get trapped at each pulse but have enough time to escape from their trap between consecutive pulses (Fig. 3(f)). As a result, the amount of trapped charges in the barrier remains weak in average but exhibits a strong time-dependent modulation. This generates an alternating stress on the oxide barrier which also leads to a shorter lifetime. This alternating stress favors atomic mobility through the barrier, i.e., pinhole formation which also yields rapid breakdown. (3) The intermediate situation with $\Delta t \sim \tau_0$ is the most favorable in terms of lifetime. The average amount of trapped electrons in the barrier is moderate as is the time-dependent modulation of this amount (Fig. 3(e)), resulting in the large observed lifetime. Since the amplitude of the charge modulation is proportional to the applied voltage, the peak around 100 ns is thus expected to decrease in magnitude for larger voltages, which is indeed observed (Figs. 3(b) and 3(c)). This overall picture is also consistent with the absence of peak when pulses of alternating polarity are used (Fig. 3(a)). Indeed, in this case, electrons are trapped and detrapped at each alternating pulses whatever the delay Δt between pulses. This yields a strong time-dependent modulation of the trapped electrons density leading therefore to a behavior similar to the one observed for pulses of same polarity when $\Delta t \gg \tau_0$.

In conclusion, charge trapping/detrapping phenomena seem to play a very important role in the aging and breakdown of MgO-based MTJs. The extremely long endurance obtained for intermediate delay times indicates that MTJ lifetime can be increased for any delay between pulses in MgO barriers by reducing the amount of trapping sites. This could be achieved by avoiding the formation of boron oxide at MgO interface, avoiding the presence of oxygen vacancies in the barrier, and obtaining a better lattice matching between magnetic electrodes and MgO to eliminate dislocations.

This work was supported by the European Commission through the ERC Adv Grant HYMAGINE.

[1]M. Hosomi, H. Yamagishi, T. Yamamoto, K. Bessho, Y. Higo, K. Yamane, H. Yamada, M. Shoji, H. Hachino, C. Fukumoto, H. Nagao, and H. Kano, IEDM Tech. Dig. 459 (2005).
[2]D. V. Dimitrov, Z. Ghao, X. Wang, W. Jung, X. Lou, and O. G. Heinonen, Appl. Phys. Lett. **94**, 123110 (2009).
[3]K. Hosotani, M. Nagamine, T. Ueda, H. Aikawa, S. Ikegawa, Y. Asao, H. Yoda, and A. Nitayama, Jpn. J. Appl. Phys. **49**, 04DD15 (2010).
[4]R. O'Connor, G. Hughes, P. Casey, and S. B. Newcomb, J. Appl. Phys. **107**, 024501 (2010).
[5]R. Takemura, T. Kawahara, K. Miura, H. Yamamoto, J. Hayakawa, N. Matsuzaki, K. Ono, M. Yamanouchi, K. Ito, H. Takahashi, S. Ikeda, H. Hasegawa, H. Matsuoka, and H. Ohno, IEEE J. Solid-State Circuits **45**, 869 (2010).
[6]J. Åckerman, P. Brown, M. DeHerrera, M. Durlam, E. Fuchs, D. Gajewski, M. Griswold, J. Janesky, J. J. Nahas, and S. Tehrani, IEEE Trans. Device Mater. Reliab. **4**, 428 (2004).
[7]J. Herault, R. C. Sousa, C. Papusoi, Y. Conraux, C. Maunoury, I. L. Prejbeanu, K. Mackay, B. Delaet, J. P. Nozieres, and B. Dieny, IEEE Trans. Magn. **44**, 2581 (2008).
[8]I. L. Prejbeanu, M. Kerekes, R. C. Sousa, H. Sibuet, O. Redon, B. Dieny, and J. P. Nozieres, J. Phys.: Condens. Matter. **19**, 23 (2007).
[9]For pulses of lower amplitude, i.e., closer to operating conditions of MRAM, the decrease of η for $\Delta t > 100$ ns is not observed (not shown), instead for these long delays, η presents a plateau and its value remains similar to its large value for $\Delta t \sim 100$ ns.
[10]D. Herranz, F. Bonell, A. Gomez-Ibarlucea, S. Andrieu, F. Montaigne, R. Villar, C. Tiusan, and F. G. Aliev, Appl. Phys. Lett. **96**, 202501 (2010).